

MHD FLOW THROUGH VARIABLE PERMEABILITY POROUS MEDIUM IN A PARALLEL PLATE CHANNEL WITH CONSTANT SUCTION AND INJECTION AT THE PLATES: A NUMERICAL INVESTIGATION

ANGAD PRASAD [✉] and P.K. SINGH

Abstract

This paper investigates the behavior of steady and fully developed magnetohydrodynamic flow in a parallel plate channel containing an incompressible, electrically conducting viscous fluid flowing through a porous medium under the influence of a uniform transverse magnetic field. The boundaries of the plates experience consistent suction and injection. The permeability of the porous medium and the viscosity of the fluid vary in the transverse direction. The Brinkman equation is utilized to describe the flow through the porous media. Numerical expressions for velocity and volumetric flow rate for two types of flows, namely Poiseuille and Couette flows, are derived using the finite difference method. The effects of various parameters such as the Hartmann number, permeability parameter, etc., on the velocity profile and volumetric flow rate are analyzed and presented graphically.

2010 *Mathematics subject classification*: 76D05; 76S05; 65L12.

Keywords and phrases: Brinkman equation, Permeability parameter, Hartmann number, Uniform suction and injection, Finite difference method.

1. Introduction

Flow through porous media is a fascinating and intricate phenomenon with widespread applications in various fields, including geology, environmental science, petroleum engineering, and civil engineering. Porous media, which can range from soil and sand to rock formations, exhibit unique characteristics that significantly influence the behavior of fluids passing through them. Understanding this phenomenon is crucial for optimizing processes such as groundwater flow, oil recovery, and filtration systems. Darcy's law, formulated by Henry Darcy in the 19th century, states that the flow rate through a porous medium is directly proportional to the pressure gradient and hydraulic conductivity, and inversely proportional to the cross-sectional area through which the fluid flows. This fundamental principle forms the basis for understanding and predicting fluid flow in porous media. Nield and Bejan's [1] renowned book,

The first author (Angad Prasad) is thankful to UGC, New Delhi, India; for providing the financial assistance (UGC-Ref. No.: 1042/(CSIR-UGC NET JUNE 2018)) to carry out this research work.

"Convection in Porous Media," offers a comprehensive overview of different alternative frameworks for analyzing fluid flow within porous materials. In 1949, Brinkman [2] introduced a modification to Darcy's equation by including an extra component termed the Brinkman term. This revised equation is commonly known as the Brinkman equation. In 1953, Berman [3] conducted groundbreaking research on laminar flow in a rectangular cross-sectional channel containing porous material, employing the perturbation method. His study marked the first significant exploration of this specific research area. Verma and Bansal [4] examined the motion of an incompressible viscous fluid confined between two parallel plates. In this setup, the upper plate maintained a constant velocity while the lower plate remained stationary, subjected to a constant suction at the stationary plate.

Fluid dynamics is a branch of physics that studies the behavior of fluids when they are in motion or at rest. One fundamental property of fluids that greatly influences their behavior is viscosity. Viscosity can be described as the resistance of a fluid to flow. The viscosity of a fluid is often assumed to remain constant, but it can actually vary based on factors such as temperature, concentration, and the presence of solid particles like ash or soot, as well as corrosion. Extensive research has focused on understanding fluid flow phenomena where viscosity is influenced by temperature variations. Variable viscosity is crucial in various fields including engineering, geophysics, biology, and meteorology, among others. Haber and Brenner [5] investigated a fluid flow situation featuring varying viscosity across space within the annular region between two concentric circular cylinders that were rotating relative to each other and were widely separated. Saikrishnan and Roy [6] investigated how temperature-dependent viscosity and the Prandtl number affect the steady, non-similar laminar forced convection flow over a rotating sphere until the separation point. They utilized an implicit finite difference scheme along with the quasi-linearization method to solve the governing equations. Verma and Datta [7] investigated magnetohydrodynamic flow within a channel featuring viscosity variations under the influence of a transverse magnetic field. They derived equations for velocity and shear stress and presented graphical representations to illustrate their findings.

Permeability refers to how easily fluids move through a porous substance, influenced by factors like pore size, shape, connectivity, and fluid properties. While in uniform and symmetrical porous materials, permeability remains consistent, natural and engineered porous systems often show differences in permeability due to variations in these factors. Forecasting fluid movement in such environments requires sophisticated modeling and characterization techniques. This area of study presents an intriguing interdisciplinary field with significant implications for hydrology, geo-sciences, environmental engineering, and bio-medicine. By deepening our comprehension of permeability discrepancies and their effects on fluid movement and transportation, researchers aim to create more precise predictive models and efficient management approaches for porous materials. Hamdan and Kamel [8] investigated the fluid flow characteristics within porous layers exhibiting variable permeability. They analyzed fluid velocity and flow rate specifically for Poiseuille flow conditions. Srivastava and Deo

[9] explored the impact of a transverse magnetic field on fluid flow within a channel filled with a viscous fluid in a porous medium, considering the variable permeability of the medium. They utilized Galerkin's techniques to derive equations describing the velocity and volumetric flow rate, focusing on both Poiseuille and Couette-Poiseuille flow configurations. Verma and Gupta [10] conducted a study on the impact of variable permeability in an annular porous region subjected to a transverse magnetic field. They employed the Galerkin method to derive numerical solutions for both velocity and volumetric flow rate.

Suction and injection techniques are crucial elements in the field of fluid mechanics across diverse industries. In industrial contexts, suction denotes the process of extracting fluid from a system, whereas injection involves the introduction of fluid into a system. These methods have broad applications across sectors such as the chemical industry, oil and gas sector, and others. Verma and Gupta [11] examined magnetohydrodynamic flow within a porous channel featuring continuous suction and injection at its boundaries, under the influence of a transverse magnetic field. They derived analytical solutions for flow velocity, flow rate, and skin friction, considering two flow configurations: Poiseuille and Couette-Poiseuille flows. Their discussion delved into the impact of different parameters on fluid velocity and flow rate. Ansari and Deo [12] investigated the effect of a magnetic field on the flow of an incompressible viscous fluid around a porous sphere situated within another porous medium. Hamza [13] investigated the impact of suction and injection on magnetohydrodynamic flow between two porous concentric cylinders filled with a porous medium. He derived an analytical solution for the velocity. Balkissoon et al. [14] explored the numerical solution for unsteady magnetohydrodynamic Poiseuille flow through a porous channel subjected to an oscillating pressure gradient using the Galerkin finite element method.

Recently, many researchers have directed their attention to exploring the problem of multi-layer porous media with variable permeability and varying viscosity. Jaiswal and Yadav [15] examined the impact of a magnetic field on the Poiseuille flow of two immiscible Newtonian fluids in a highly porous medium. They investigated various viscosities and permeabilities in different regions and assessed how parameters such as permeability, porosity, and magnetic number affect the velocity profile and flow rate. Zaytoon and Hamdan [16] investigated the two-layer flow of a fluid characterized by pressure-dependent viscosity and variable permeability within an inclined porous channel. Maurya and Deo [17] investigated the impact of a magnetic field on the flow dynamics of a Newtonian fluid trapped between two micropolar fluids within a porous cylindrical shells. They derived analytical solutions for velocity profiles and volumetric flow rates as affected by this magnetic field. Yadav et al. [18] investigated the fluid dynamics within a horizontal channel containing three separate porous layers. They utilized different permeability functions to characterize the flow behavior within each of these porous zones. Maurya and Deo [19] explored how a magnetic field affects the flow of Jeffery and Newtonian fluids within a composite porous channel. Yadav and Verma [20] conducted research on the behavior of two immiscible viscous fluids

with viscosity that varies within an inclined channel. They derived exact solutions for velocity and flow rate. Numerous researchers [21–24] have recently carried out studies on mathematical modeling and the Homotopy Analysis Method within the field of fluid mechanics.

Earlier some studies have explored magnetohydrodynamic fluid flow issues with suction and injection occurring at the channel walls. The novelty of the present work lies in the application of the finite difference method to a fluid flow problem involving suction and injection, where both the permeability of the porous medium and the viscosity of the fluid undergo nonlinear variations. In this paper, we explore the numerical approach to solving magnetohydrodynamic fluid dynamics in a parallel plate channel containing a porous medium, with constant suction and injection at the walls. The permeability of the porous medium and the fluid viscosity exhibit nonlinear variations across the transverse direction. Both Poiseuille and Couette-Poiseuille flows are examined. We visually illustrate the impact of the Hartmann number, permeability parameter, and suction and injection parameter on velocity and flow rate for both flow scenarios.

2. Mathematical Formulation

Let's consider a situation where an incompressible, electrically conductive viscous fluid is steadily flowing within a parallel plate channel. The channel contains a porous medium, and the permeability of this porous medium varies in the direction perpendicular to the flow. In other words, the permeability of the porous medium is not constant throughout the channel. The flow has reached a stable state known as fully developed flow. The flow within the channel is propelled by a constant applied pressure gradient, denoted as $\frac{\partial \tilde{p}}{\partial \tilde{x}}$, acting along the \tilde{X} -axis. Additionally, there is a uniform magnetic field \tilde{B} applied perpendicular to the plates, in the direction of the \tilde{Y} -axis. It is assumed that the magnetic Reynolds number is exceedingly small, resulting in negligible induced current. Furthermore, no external electric field is present, implying that any internal phenomena such as charge separation or polarization do not contribute to an induced electric field. The fluid is introduced into the parallel channel through the lower wall with a constant velocity \tilde{V} along the \tilde{Y} -axis, while fluid particles are extracted from the channel at the same velocity \tilde{V} through the upper wall, as depicted in Fig. 1. Additionally, we consider that the induced magnetic field can be disregarded when compared to the applied magnetic field. As a result, the governing equation describing the flow is Brinkman equation, which can be expressed as [11]:

$$\tilde{\mu}_e \frac{d^2 \tilde{u}}{d\tilde{y}^2} - \tilde{\rho} \tilde{V} \frac{d\tilde{u}}{d\tilde{y}} - \frac{\tilde{\mu}}{\tilde{k}} \tilde{u} - \tilde{\sigma} \tilde{B}^2 \tilde{u} = \frac{\partial \tilde{p}}{\partial \tilde{x}}, \quad (2.1)$$

where \tilde{u} , $\tilde{\mu}$, $\tilde{\rho}$, $\tilde{\sigma}$ represent the velocity, viscosity, density, and electrical conductivity of the fluid, respectively. In this equation, \tilde{k} is the permeability of the porous medium, $\tilde{\mu}_e$ is the effective viscosity of the fluid in a porous medium and \tilde{V} is the

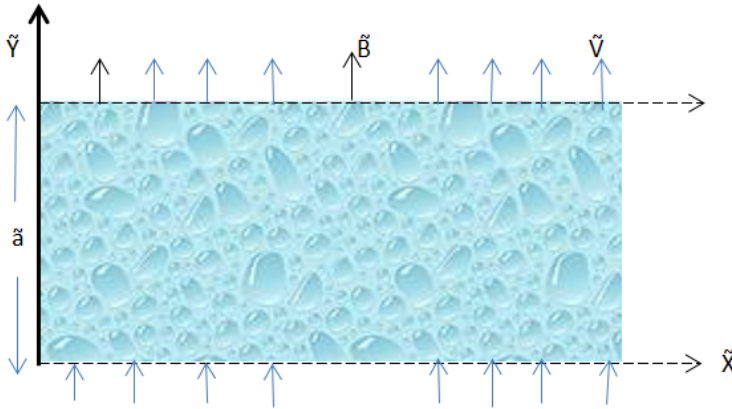


FIGURE 1. Physical model of the problem

constant suction/injection velocity. We assume that $\tilde{\mu}_e = \tilde{\mu}$ for high porosity with this assumption Eq. (2.1) becomes

$$\frac{d^2\tilde{u}}{d\tilde{y}^2} - \frac{\tilde{\rho}\tilde{V}}{\tilde{\mu}} \frac{d\tilde{u}}{d\tilde{y}} - \frac{\tilde{u}}{\tilde{k}(y)} - \frac{\tilde{\sigma}\tilde{B}^2\tilde{u}}{\tilde{\mu}} = \frac{1}{\tilde{\mu}} \frac{\partial\tilde{p}}{\partial\tilde{x}}. \tag{2.2}$$

The permeability of the porous medium is described by the function $\tilde{k}(y) = \tilde{k}_0(1 - \epsilon y)^3$, where \tilde{k}_0 represents the characteristic permeability of the medium and the parameter ϵ ranges between 0 and 1. When $\epsilon = 0$ the permeability of the porous medium remains constant. Similarly, the viscosity of the fluid within the porous medium is described by $\tilde{\mu}(y) = \tilde{\mu}_0(1 - \delta y^2)$, where $\tilde{\mu}_0$ is the constant viscosity of the fluid and the parameter δ varies between 0 and 1. If δ equals 0, the fluid viscosity remains constant. The permeability of the porous media and the viscosity of the fluid are controlled by the two parameters, ϵ and δ , respectively.

Introducing the following dimensionless variables

$$u = \frac{\tilde{u}}{\tilde{U}}, \quad y = \frac{\tilde{y}}{\tilde{a}}, \quad P = -\frac{\tilde{a}^2}{\tilde{\mu}_0\tilde{U}} \frac{\partial\tilde{p}}{\partial\tilde{x}},$$

where \tilde{U} is the characteristic velocity and \tilde{a} is the distance between the plates of the channel. Now Eq. (2.2) becomes

$$\frac{d^2u}{dy^2} - \frac{S}{(1 - \delta y^2)} \frac{du}{dy} - \left(\frac{\alpha^2}{(1 - \epsilon y)^3} + \frac{M^2}{(1 - \delta y^2)} \right) u = -\frac{P}{(1 - \delta y^2)}, \tag{2.3}$$

where $S = \frac{\tilde{\rho}\tilde{a}\tilde{V}}{\tilde{\mu}_0}$ is suction/injection Parameter, $\alpha = \frac{\tilde{a}}{\sqrt{\tilde{k}_0}}$ is permeability parameter and $M = \sqrt{\frac{\tilde{\sigma}\tilde{B}^2\tilde{a}^2}{\tilde{\mu}_0}}$ is Hartmann number.

3. Numerical Solution of the Problem

The finite difference method is a numerical technique used for solving differential equations by approximating them with a set of discrete difference equations. It involves dividing the spatial and/or temporal domain into a grid or mesh of discrete points, and then approximating the derivatives in the differential equations using finite difference approximations. These approximations relate the function values at neighboring grid points, allowing the differential equation to be transformed into a system of algebraic equations. The resulting system is then solved numerically to obtain an approximation of the solution to the original differential equation. Finite difference methods are widely used in various fields such as physics, engineering, and finance for solving partial differential equations and ordinary differential equations in both one and multiple dimensions.

The finite difference method is applied for solving the Eq. (2.3), the symmetric derivative formulae at the j^{th} node,

$$\frac{du}{dy} = \frac{u_{j+1} - u_{j-1}}{2h}, \tag{3.1}$$

$$\frac{d^2u}{dy^2} = \frac{u_{j+1} - 2u_j + u_{j-1}}{h^2}. \tag{3.2}$$

Employing this difference approximation in the Eq. (2.3)

$$\frac{u_{j+1} - 2u_j + u_{j-1}}{h^2} - \frac{S}{(1 - \delta y_j^2)} \frac{u_{j+1} - u_{j-1}}{2h} - \left(\frac{\alpha^2}{(1 - \epsilon y_j)^3} + \frac{M^2}{(1 - \delta y_j^2)} \right) u_j = - \frac{P}{(1 - \delta y_j^2)}, \tag{3.3}$$

where, $y_j = 0 + (j - 1)h$. Rearranging the term of the above equation

$$\left(\frac{1}{h^2} + \frac{S}{2h(1 - \delta y_j^2)} \right) u_{j-1} - \left(\frac{2}{h^2} + \frac{\alpha^2}{(1 - \epsilon y_j)^3} + \frac{M^2}{(1 - \delta y_j^2)} \right) u_j + \left(\frac{1}{h^2} - \frac{S}{2h(1 - \delta y_j^2)} \right) u_{j+1} = - \frac{P}{(1 - \delta y_j^2)}. \tag{3.4}$$

3.1. Poiseuille flow In Poiseuille flow, the flow within the channel is induced by a consistent applied pressure gradient, while both the top and bottom surfaces of the channel remain stationary. The boundary condition at these plates, where the fluid adheres to the surface due to the no-slip condition, is expressed in a dimensionless form:

$$\left. \begin{aligned} u &= 0, \text{ at } y = 0 \\ u &= 0, \text{ at } y = 1 \end{aligned} \right\},$$

discretized this condition

$$\left. \begin{array}{l} u_j = 0, \text{ at } j = 1 \\ u_j = 0, \text{ at } j = n + 1 \end{array} \right\} .$$

Substituting $j = 2, 3, 4, \dots, n$. in the equation Eq. (3.4) with this boundary equation. we will get the system of algebraic equation which can be solved by Mathematical tool Matlab in the form of graphs.

3.2. Couette-Poiseuille flow In Couette-Poiseuille flow, the flow within the channel is generated by a constant applied pressure gradient. In this flow configuration, one plate of the channel is kept stationary, while the other plate is set in motion with a constant velocity.

$$\left. \begin{array}{l} u = 0, \text{ at } y = 0 \\ u = 1, \text{ at } y = 1 \end{array} \right\} ,$$

discretized this condition

$$\left. \begin{array}{l} u_j = 0, \text{ at } j = 1 \\ u_j = 1, \text{ at } j = n + 1 \end{array} \right\}$$

Substituting $j = 2, 3, 4, \dots, n$. in the equation Eq. (3.4) with this boundary equation. we will get the system of algebraic equation which can be solved by Mathematical tool Matlab in the form of graphs.

4. Volumetric Flow Rate

The volumetric flow rate Q for the channel is defined as:

$$Q = \int_0^1 u dy = \int_0^1 u_j dy. \quad (4.1)$$

By putting the value of fluid velocity in different interval, the volumetric flow rate can be evaluated.

5. Result and Discussion

The research examines the behavior of Poiseuille and Couette-Poiseuille flows within a parallel plate channel filled with an incompressible, electrically conducting fluid, under the influence of a uniform magnetic field. The flow through porous media is modeled using the Brinkman equation. The finite difference method is employed for obtaining numerical solutions. Computational simulations are performed using Matlab, with the domain defined as $0 \leq y \leq 1$ and a grid size h set to 0.025, resulting in the partitioning of the domain into 40 equal segments. The velocities u_j for $j = 2, 3, \dots, 40$ are computed numerically and presented graphically.

5.1. Analysis of velocity profile with different parameters In this section, we will explore the influence of different parameters on the fluid velocity. Figure 2 depicts

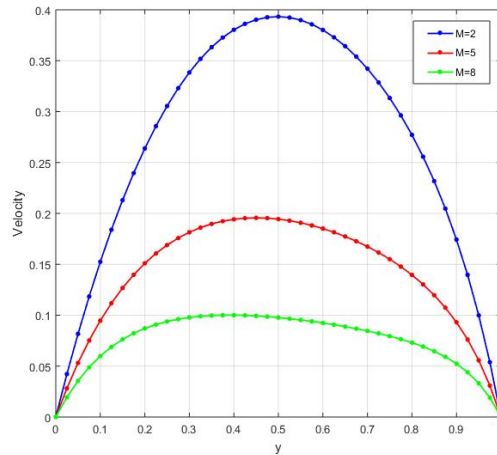


FIGURE 2. Impact of the Hartmann number M on the velocity profile where the parameters are fixed at $P = 5$, $S = 2$, $\alpha = 2$, $\epsilon = 0.5$, and $\delta = 0.4$ in the Poiseuille flow.

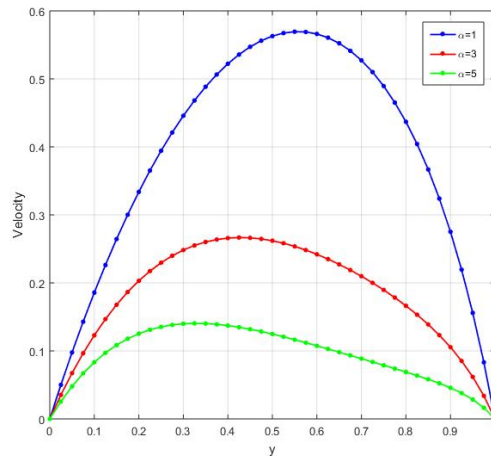


FIGURE 3. Impact of the Permeability parameter α on the velocity profile where the parameters are fixed at $P = 5$, $S = 2$, $M = 2$, $\epsilon = 0.5$, and $\delta = 0.4$ in the Poiseuille flow.

the influence of various values of Hartmann numbers M on the velocity profile in Poiseuille flow, while keeping other parameters constant. The illustration suggests that as the Hartmann number rises, the fluid velocity decreases. This phenomenon can be attributed to the heightened Hartmann number, indicating an increase in the magnetic field strength, which consequently diminishes the fluid velocity. Figure 3 illustrates the effect of varying permeability parameter α on the velocity profile in Poiseuille

flow, while maintaining other parameters constant. The graph demonstrates that as the permeability parameters increase, the fluid velocity decreases. This trend can be explained by the higher permeability parameters indicating a reduction in permeability, which subsequently lowers the fluid velocity.

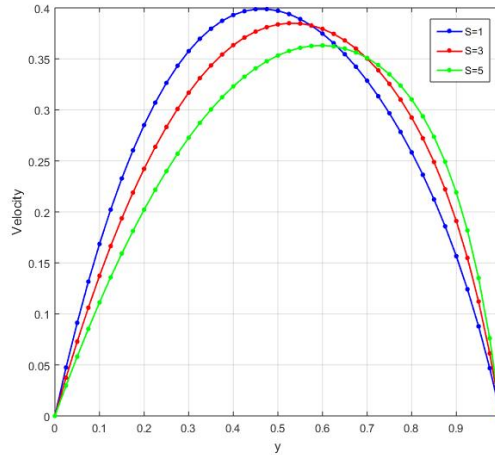


FIGURE 4. Impact of the Suction injection parameter S on the velocity profile where the parameters are fixed at $P = 5$, $M = 2$, $\alpha = 2$, $\epsilon = 0.5$, and $\delta = 0.4$ in the Poiseuille flow.

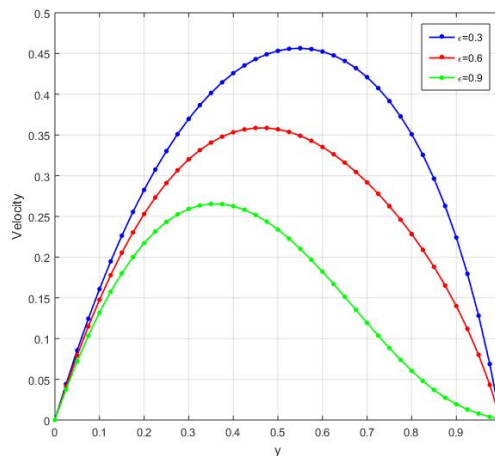


FIGURE 5. Impact of the ϵ on the velocity profile where the parameters are fixed at $P = 5$, $S = 2$, $M = 2$, $\alpha = 2$, and $\delta = 0.4$ in the Poiseuille flow.

Figure 4 illustrates the effect of different values of suction injection parameter S on the velocity profile in Poiseuille flow, while maintaining other parameters constant. The graph demonstrates that as the suction injection parameter increase, the fluid

velocity decreases. Figure 5 displays the effect of different values of the parameter ϵ on the velocity profile in Poiseuille flow, with all other parameters held constant. The graph demonstrates that as the ϵ increase, the fluid velocity decreases. This trend can be explained by the higher values of the ϵ indicating a reduction in permeability, which subsequently lowers the fluid velocity.

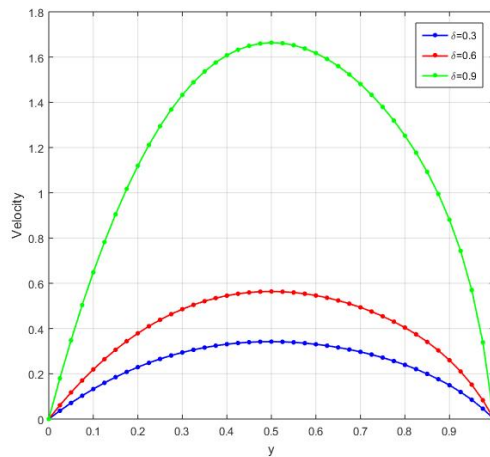


FIGURE 6. Impact of the δ on the velocity profile where the parameters are fixed at $P = 5, S = 2, M = 2, \alpha = 2,$ and $\epsilon = 0.5$ in the Poiseuille flow.

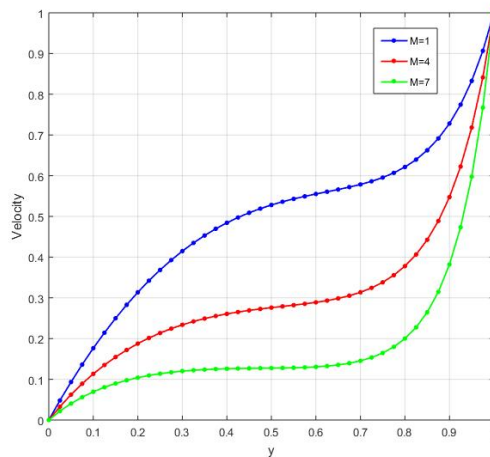


FIGURE 7. Impact of the Hartmann number M on the velocity profile where the parameters are fixed at $P = 5, S = 2, \alpha = 2, \epsilon = 0.5,$ and $\delta = 0.4$ in the Couette-Poiseuille flow.

Figure 6 displays the effect of different values of the parameter δ on the velocity profile in Poiseuille flow, while maintaining other parameters constant. The graph demonstrates that as the δ increase, the fluid velocity increases. This trend can be

explained by the higher values of the δ indicating a reduction in viscosity, which subsequently increases the fluid velocity. Figure 7 illustrates how the velocity profile

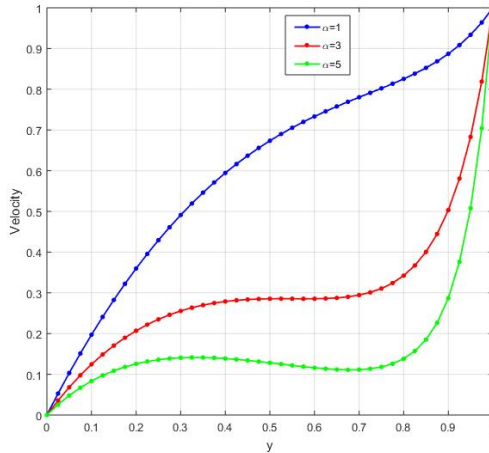


FIGURE 8. Impact of the Permeability parameter α on the velocity profile where the parameters are fixed at $P = 5, S = 2, M = 2, \epsilon = 0.5$, and $\delta = 0.4$ in the Couette-Poiseuille flow.

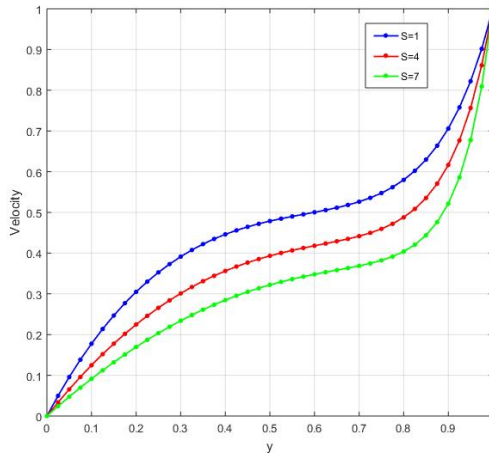


FIGURE 9. Impact of the Suction injection parameter S on the velocity profile where the parameters are fixed at $P = 5, M = 2, \alpha = 2, \epsilon = 0.5$, and $\delta = 0.4$ in the Couette-Poiseuille flow.

in Couette-Poiseuille flow changes with different Hartmann numbers M , with all other factors held constant. The visualization implies that as the Hartmann number increases, the fluid velocity decreases. This observation can be explained by the fact that higher Hartmann numbers signify stronger magnetic fields, which in turn reduce the fluid velocity. Figure 8 depicts how changes in permeability parameter α affect the velocity profile in Couette-Poiseuille flow, with other factors held constant. The graph

shows that as permeability parameters increase, fluid velocity decreases. This pattern can be attributed to higher permeability parameters indicating reduced permeability, leading to a decrease in fluid velocity. Figure 9 shows how various values of suction

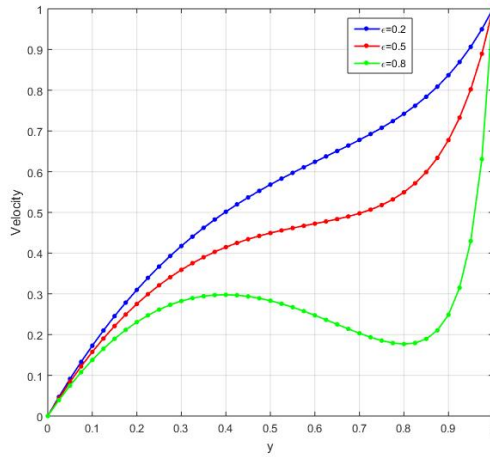


FIGURE 10. Impact of the ϵ on the velocity profile where the parameters are fixed at $P = 5, S = 2, M = 2, \alpha = 2$, and $\delta = 0.4$ in the Couette-Poiseuille flow.

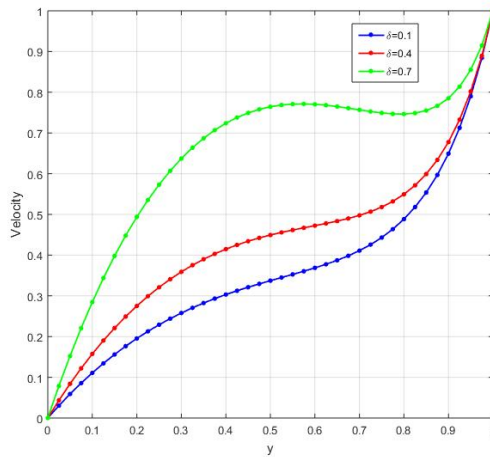


FIGURE 11. Impact of the δ on the velocity profile where the parameters are fixed at $P = 5, S = 2, M = 2, \alpha = 2$, and $\epsilon = 0.5$ in the Couette-Poiseuille flow.

injection parameter S impact the velocity profile in Couette-Poiseuille flow, with all other factors remaining unchanged. The graph indicates that as the suction injection parameters increase, the fluid velocity decreases. Figure 10 illustrates how varying values of the parameter ϵ impact the velocity profile in Couette-Poiseuille flow, while keeping all other parameters constant. The graph shows that as ϵ increases, fluid

velocity decreases. This trend can be attributed to higher values of ϵ indicating reduced permeability, which leads to a decrease in fluid velocity. Figure 11 illustrates how varying values of the parameter δ affect the velocity profile in Couette-Poiseuille flow, with all other parameters held constant. The graph shows that as δ increases, fluid velocity increases. This pattern can be explained by higher values of δ suggesting reduced viscosity, resulting in an increase in fluid velocity.

5.2. Analysis of volumetric flow rate with different parameters In this section, we will explore the influence of different parameters on the volumetric flow rate.

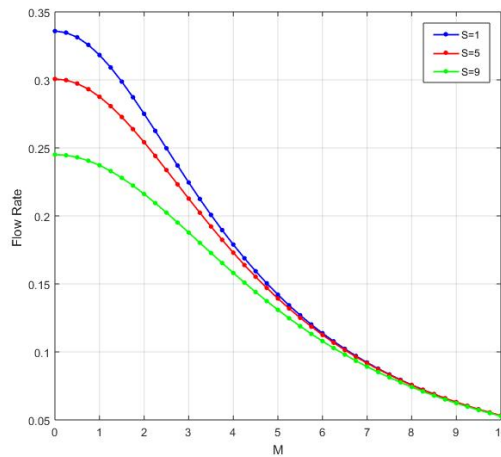


FIGURE 12. Impact of the Suction injection parameter S with Hartmann number M on the volumetric flow rate where the parameters are fixed at $P = 5$, $\alpha = 2$, $\epsilon = 0.5$, and $\delta = 0.4$.

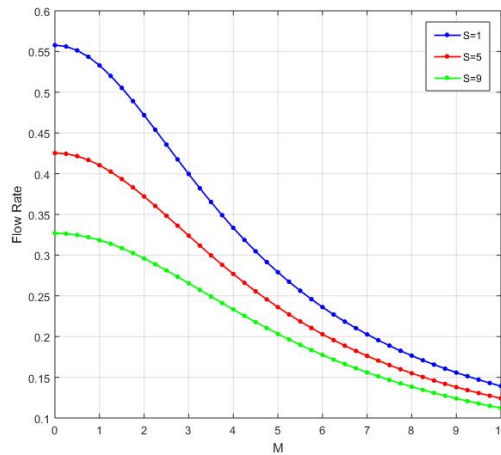


FIGURE 13. Impact of the Suction injection parameter S with Hartmann number M on the volumetric flow rate where the parameters are fixed at $P = 5$, $\alpha = 2$, $\epsilon = 0.5$, and $\delta = 0.4$.

Figure 12 and Figure 13 illustrates how the volumetric flow rate changes with the Hartmann number and the suction injection parameter in Poiseuille flow and Couette-Poiseuille flow respectively. These demonstrate that as the Hartmann number increases, indicating a stronger presence of resistive Lorentz force, the flow rate decreases. Additionally, the figure indicates that lower values of the suction injection parameter result in higher volumetric flow rates.

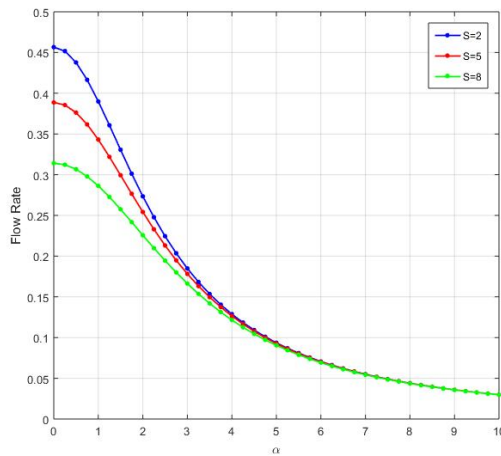


FIGURE 14. Impact of the Suction injection parameter S with permeability parameter α on the volumetric flow rate where the parameters are fixed at $P = 5$, $M = 2$, $\epsilon = 0.5$, and $\delta = 0.4$.

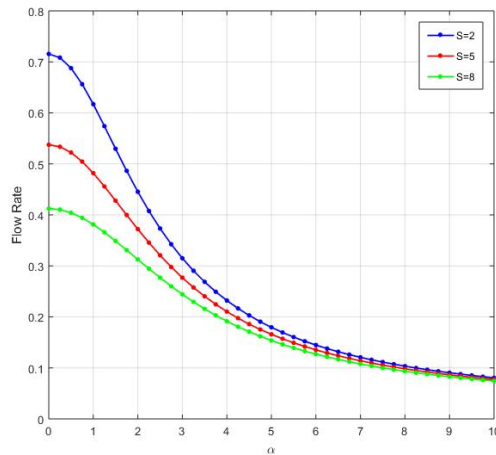


FIGURE 15. Impact of the Suction injection parameter S with permeability parameter α on the volumetric flow rate where the parameters are fixed at $P = 5$, $M = 2$, $\epsilon = 0.5$, and $\delta = 0.4$.

Figure 14 and Figure 15 illustrates the relationship between volumetric flow rate, permeability parameter, and suction injection parameter in Poiseuille flow and Couette-Poiseuille flow respectively. These show that as the permeability parameter increases, indicating a decrease in permeability, the flow rate decreases. Additionally, the figure indicates that lower values of the suction injection parameter result in higher volumetric flow rates.

6. Conclusion

In this study, a numerical approximation is used to analyze the behavior of steady and fully developed magnetohydrodynamic flow in a parallel plate channel containing a porous medium with constant suction and injection at the plates. The permeability of the porous medium and viscosity of the fluid exhibit nonlinear variation across the transverse direction. Two types of flows are considered namely Poiseuille flow and Couette-Poiseuille flow. Numerical expressions for fluid velocity and volumetric flow rate have been obtained. The effects of various parameters, such as the Hartmann number, permeability parameter, etc., on the velocity profile and volumetric flow rate have been plotted and discussed. This study will help researchers obtain numerical solutions when some physical quantity undergoes nonlinear variations. The application scope of this problem is extensive, spanning across various fields including water filtration systems, magnetohydrodynamic generators, air purification systems, water cooling mechanisms, arterial blood flow dynamics, petroleum, and chemical engineering. Based on the analysis presented earlier, the following conclusions can be inferred:

- The Hartmann number, permeability parameter, and suction injection parameter all contribute to decreasing fluid velocity in both Poiseuille and Couette-Poiseuille flows.
- The parameter δ increases fluid velocity in both Poiseuille and Couette-Poiseuille flows.
- The parameter ϵ decreases fluid velocity in both Poiseuille and Couette-Poiseuille flows.
- The Hartmann number, permeability parameter, and suction and injection parameter all lead to a reduction in the flow rate.

Author contributions:

Conceptualisation: P.K. Singh, Angad Prasad ; *Software:* Angad Prasad ; *Writing-Original Draft:* Angad Prasad

Conflicts of Interest: The authors declare no conflict of interest.

References

- [1] D.A. Nield and A. Bejan, *Convection in porous media*, 3rd edition Springer (2006).
- [2] H.C. Brinkman, *A calculation of the viscous force exerted by a flowing fluid on a dense swarm of particles*, Appl. Sci. Res. **A1** (1949) 27–34.
- [3] A.S. Berman, *Laminar flow in channel with porous walls*, J. Appl. Phys. **24** (1953) 1232–1235.
- [4] P.D. Verma and J.L. Bansal, *Flow of a viscous incompressible fluid between two parallel plates: one in uniform motion and other at rest with uniform at the stationary plate*, Proc. Indian Acad. of Sci. **64 A** (1966) 385–396.
- [5] S. Haber and H. Brenner, *Inhomogeneous viscosity fluid flow in a wide-gap couette apparatus: shear-induced migration in suspensions*, Phys. of Fluids **12** (2000) 3100–3111.
- [6] P. Saikrishnan and S. Roy, *Steady non similar axisymmetric water layers with variable viscosity and Prandtl Number*, Acta Mechanica **157** (2002) 187–199.
- [7] V.K. Verma and S.Datta, *Magnetohydrodynamic flow in a channel with varying viscosity under transverse magnetic field*, Adv. Theoret. Appl. Mech. **3** (2010) 53–66.
- [8] M.H. Hamdan and M.T. Kamel, *Flow through variable porous layers*, Adv.Theor. Appl. Mech. **4** (2011) 135–145.
- [9] B.G. Srivastava and S. Deo, *Effect of magnetic field on the viscous fluid flow in a channel with porous medium of variable permeability*, Appl. Math. comput. **219** (2013) 8959–8964.
- [10] V.K. Verma and A.K. Gupta, *Brinkman flow of a conducting fluid in an annular porous channel of variable permeability in the presence of magnetic field*, Ganita **66** (2016) 93–104.
- [11] V.K. Verma and A.K. Gupta, *MHD flow in porous channel with constant suction/injection at the walls*, Int. J. pure appl. Math. **118** (2018) 111–123.
- [12] I.A. Ansari and S. Deo, *Magnetohydrodynamic viscous fluid flow past a porous sphere embedded in another porous medium*, Spec. Top. Rev. Porous Media **9** (2018) 191–200.
- [13] S.E.E. Hamza, *The effect of suction and injection on MHD flow between two porous concentric cylinders filled with porous medium*, J. Adv. Phys. **16** (2019) 156–170.
- [14] J.N. Balkissoon, S.R. Gunakala and V.M. Job, *Unsteady MHD Poiseuille flow through a porous channel under an oscillating pressure gradient and uniform suction/injection*, The Int. Conf. on Emerg. Trends in Eng. and Tech. (2020) 86–95.
- [15] S. Jaiswal and P.K. Yadav, *Influence of magnetic field on the Poiseuille flow of immiscible Newtonian fluid through highly porous medium*, J. of the Brazilian Society of Mech. Sci. and Eng. **42** (2020) 188.
- [16] M.S.A. Zaytoon and M.H. Hamdan, *Fluid mechanics at the interface between a variable viscosity fluid layer and a variable permeability porous medium*, Wseas Trans. Heat Mass Transfer **16** (2021) 159–169.
- [17] D.K. Maurya and S. Deo, *Effect of magnetic field on Newtonian fluid sandwiched between non-Newtonian fluids through porous cylindrical shells*, Spec. Topics Rev. Porous Media **13** (2022) 75–92.
- [18] P.K. Yadav, S.Jaiswal, A.K. Verma, and A.J. Chamkha, *MHD of immiscible Newtonian fluids in porous regions of different variable permeability functions*, J. Petr. Sci. Eng. **220**, part B, (2023).
- [19] P.K. Maurya and S. Deo, *Influence of magnetic field on the flow of Jeffery and Newtonian fluids through composite porous channel*, Spec. Top. Rev. Porous Media **14** (2023) 49–60.
- [20] P.K. Yadav and A.K. Verma, *Analysis of the MHD flow of immiscible fluids with variable viscosity in an inclined channel*, J. Appl. Mech. Tech. Phys. **64** (2023) 618–627.
- [21] P.K. Yadav and M. Roshan, *Mathematical modeling of blood flow in an annulus porous region between two coaxial deformable tubes: an advancement to peristaltic endoscope*, Chinese Journal of Physics **88** (2024) 89–109.
- [22] P.K. Yadav and M. Roshan, *Mathematical modeling of creeping electromagnetohydrodynamic peristaltic propulsion in an annular gap between sinusoidally deforming permeable and impermeable curved tubes*, Physics of Fluids **36** (2024) 071907(1–19).
- [23] P.K. Yadav and N. Yadav, *Impact of heat and mass transfer on the magnetohydrodynamic two-phase flow of couple stress fluids through a porous walled curved channel using Homotopy*

- analysis method*, Chaos Solitons and Fractals **183** (2024) 114961.
- [24] P.K. Yadav and N. Yadav, *Magnetohydrodynamic study of micropolar fluid flow in the porous walled channel with variable viscosity and thermal conductivity: HAM solution*, Chaos Solitons and Fractals **181** (2024) 114726.

ANGAD PRASAD, Department of Mathematics
University of Allahabad, Prayagraj-211002 (U.P.) India.
e-mail: angad.p@allduniv.ac.in

P.K. SINGH, Department of Mathematics
University of Allahabad, Prayagraj-211002 (U.P.) India.
e-mail: pramod_ksingh@allduniv.ac.in